Journal of Solid State Chemistry 184 (2011) 3117–3120

Contents lists available at SciVerse ScienceDirect

Journal of Solid State Chemistry

journal homepage: www.elsevier.com/locate/jssc

Synthesis, structure and physical properties of reduced barium titanate $Ba_2Ti_{13}O_{22}$

Kunimitsu Kataoka [a,b,*,1], Norihito Kijima [a], Hiroshi Hayakawa [a], Akira Iyo [a], Ken-ichi Ohshima [b], Junji Akimoto [a]

[a] National Institute of Advanced Industrial Science and Technology (AIST), 1-1-1 Higashi, Tsukuba, Ibaraki 305-8565, Japan
[b] Graduate School of Pure and Applied Sciences, University of Tsukuba, 1-1-1 Tennodai, Tsukuba, Ibaraki 305-8573, Japan

ARTICLE INFO

Article history:
Received 5 March 2011
Received in revised form
5 September 2011
Accepted 11 September 2011
Available online 17 September 2011

Keywords:
Oxides
X-ray diffraction
Electrical conductivity

ABSTRACT

Polycrystalline sample of the reduced barium titanate $Ba_2Ti_{13}O_{22}$ was synthesized by solid state reaction at 1523 K in Ar atmosphere for the first time. The Rietveld refinement using the powder X-ray diffraction data confirmed the sample to be main phase of $Ba_2Ti_{13}O_{22}$ having the orthorhombic crystal system, space group *Bmab* and the lattice parameters of $a=11.67058(11)$ Å, $b=14.12020(13)$ Å and $c=10.06121(9)$ Å, and $V=1657.995(20)$ Å^3. The valence state of Ti was evaluated by both the Ti–O bond distance analysis and the Ti K-edge XANES analysis. The magnetic susceptibility was nearly temperature independent in the range of 60–300 K, suggesting the Van Vleck Paramagnetism. The electrical conductivity at 300 K is approximately 320.50 S/cm, and a semiconducting behavior was observed below room temperature. The Seebeck coefficient showed a negative value of -1.25 μV/K at 300 K, indicating *n*-type behavior. These facts were confirmed by the results of the present theoretical calculations by the FLAPW method.

1. Introduction

The reduced titanium oxides in the A–Ti^{3+}–Ti^{4+}–O (A: alkali or alkaline-earth metal) system display interesting magnetic and electronic properties. For example, the spinel-type $LiTi_2O_4$ is oxide superconductor [1], and the calcium ferrite-type $NaTi_2O_4$ is known to display anomaly magnetic susceptibility for Ti^{3+}–Ti^{3+} spin correlations [2].

In the Ba–Ti^{3+}–Ti^{4+}–O system, six structure-types were reported in the literature; hexagonal $BaTiO_{3-\delta}$ [3,4], $Ba_2Ti_{13}O_{22}$ [5,6], $Ba_2Ti_6O_{13}$ [7], tetragonal and monoclinic forms of $Ba_xTi_8O_{16}$ [8,9] and $Ba_4Ti_{12}O_{27}$ [10]. In these compounds, $Ba_2Ti_{13}O_{22}$ is most reduced barium titanate; the chemical formula can be also represented as $Ba_2Ti_{12}^{3+}Ti^{4+}O_{22}$, so the interesting electrical properties were expected. Previously, small single crystal samples of $Ba_2Ti_{13}O_{22}$ were synthesized by two independent research groups, and the crystal structure was determined by single-crystal X-ray diffraction technique [5,6]. In addition, temperature dependence of magnetic susceptibility using the single-crystal samples was reported [6]. However, the sintered polycrystalline samples of $Ba_2Ti_{13}O_{22}$ for the purpose of revealing the conduction properties have not been synthesized yet, to our knowledge.

In the present study, we prepared the polycrystalline samples of $Ba_2Ti_{13}O_{22}$ by solid state reaction, and characterized by powder X-ray diffraction. The valence state of Ti in $Ba_2Ti_{13}O_{22}$ was examined by both the Ti–O bond distance analysis and the Ti K-edge XANES spectra. Furthermore, the physical properties including electrical conductivity were clarified for the first time. The results were compared with the theoretical calculations.

2. Experimental procedure

A polycrystalline sample of $Ba_2Ti_{13}O_{22}$ was prepared by solid-state reaction:

$$Ba_2TiO_4+9TiO_2+Ti\rightarrow Ba_2Ti_{13}O_{22}.$$

The starting materials were Ba_2CO_3 (purity: 99.9%), TiO_2 (purity: 99.9%) and Ti metal (purity: 99.9%). Ba_2TiO_4 was first prepared by firing $BaCO_3$ and TiO_2 in the correct proportion at 1423 K for 72 h in air. A mixture of Ba_2TiO_4, TiO_2 and Ti in a molar ratio of 1:9:1 was pressed into a pellet, placed in an iron crucible, and heated in a resistance furnace at 1523 K in an argon gas flow for 16 h.

The phase purity and crystal structure of the obtained sample were characterized by powder X-ray diffraction (XRD) profiles

* Corresponding author at: National Institute of Advanced Industrial Science and Technology (AIST), 1-1-1 Higashi, Tsukuba, Ibaraki 305-8565, Japan.
E-mail address: kataoka-kunimitsu@aist.go.jp (K. Kataoka).
[1] Research Fellow of the Japan Society for the Promotion of Science.

0022-4596/$ - see front matter © 2011 Elsevier Inc. All rights reserved.
doi:10.1016/j.jssc.2011.09.008

measured at room temperature with Cu $K\alpha$ radiation using a Rigaku RINT2550V diffractometer (operating conditions: 40 kV, 200 mA) equipped with a curved graphite monochromator. The XRD intensity data were collected for 1 s at each 0.03° step over a 2θ range from 5° to 140° for Rietveld analysis.

The chemical composition was verified by scanning electron microscopy-energy dispersive X-ray (SEM-EDX) analysis (JEOL JSM-5400).

The Ti K-edge X-ray absorption near-edge structure (XANES) spectra of $Ba_2Ti_{13}O_{22}$ were measured in the transmission mode at room temperature. The experiments were carried out at BL-9A, Photon Factory, KEK, Japan. Ti foil was used to calibrate the energy of the Ti K-edge.

The electrical conductivity of $Ba_2Ti_{13}O_{22}$ was measured using the sintered sample from 13 to 300 K by a conventional direct-current four probe method. The thermoelectric power of the sintered $Ba_2Ti_{13}O_{22}$ samples was measured at 300 K by a comparative technique using a constantan standard with a Seebeck measurement system (MMR Technologies, Inc., SB-100). The magnetic susceptibility measurements were performed using a superconducting quantum interference device (SQUID) magnetometer (Quantum Design, MPMS) under field cooling at 1 kOe of external magnetic field, in the temperature range from 301 K to 5 K.

The electronic structure and electron density distribution (EDD) of $Ba_2Ti_{13}O_{22}$ were calculated using the full-potential linearized augmented-plane-wave (FLAPW) method with the WIEN2k program [11]. The localized spin density approximation (LSDA) with Hubbard U (LSDA+U, U=4.0 eV) in the formulation of Kohn and Sham was used for exchange and correlation terms [12]. The atomic muffin-tin sphere radii of the Ba, O, and Ti atoms were 2.50 a.u., 1.95 a.u. and 1.73 a.u., respectively. The plane-wave cutoff was $R_{MT} \times K_{max}$=7.0, where R_{MT} is the smallest atomic sphere radius in the unit cell and K_{max} is the magnitude of the largest k vector. Self-consistency was carried out on a 400 k-point mesh in the full Brillouin zone. The energy criterion for self-consistency was set to less than 0.001 eV per formula unit. The present structural parameters of $Ba_2Ti_{13}O_{22}$ were used in the calculation. The obtained electron density distributions were drawn with the VESTA program [13].

3. Results and discussion

3.1. Synthesis and chemical characterization

Powder X-ray diffraction data revealed the black polycrystalline sample of solid state reaction at 1523 K to be a single phase of $Ba_2Ti_{13}O_{22}$. EDX analysis showed that the product was barium titanate and was free from Fe contamination from the crucible. The obtained sample was identified to be a main phase of $Ba_2Ti_{13}O_{22}$, orthorhombic crystal system and space group *Bmab*. The lattice parameters for the present $Ba_2Ti_{13}O_{22}$ sample were refined by the Rietveld refinement using the XRD data to be a=11.67058(11) Å, b=14.12020(13) Å and c=10.06121(9) Å, and V=1657.995(20) Å^3. These values were in good agreement with those for the previous single-crystal data [6]. The sample was contained small amounts of $Ba_2Ti_6O_{13}$ and TiO_2 as impurities.

The valence state of Ti in $Ba_2Ti_{13}O_{22}$ was also examined by the Ti K-edge XANES spectrum, as shown in Fig. 1. The spectrum was compared with those of Ti_2O_3 and TiO_2 as reference materials in Fig. 1, in which the valence states of Ti are 3+ and 4+, respectively. The chemical shift in the XANES spectra has a positive correlation with the valence states of the absorber atom. As can be seen in Fig. 1, the main inflection (4960–5000 eV) of Ti for $Ba_2Ti_{13}O_{22}$ is very close to that of Ti_2O_3. This fact strongly suggests that the valence state of Ti in $Ba_2Ti_{13}O_{22}$ is close to 3+.

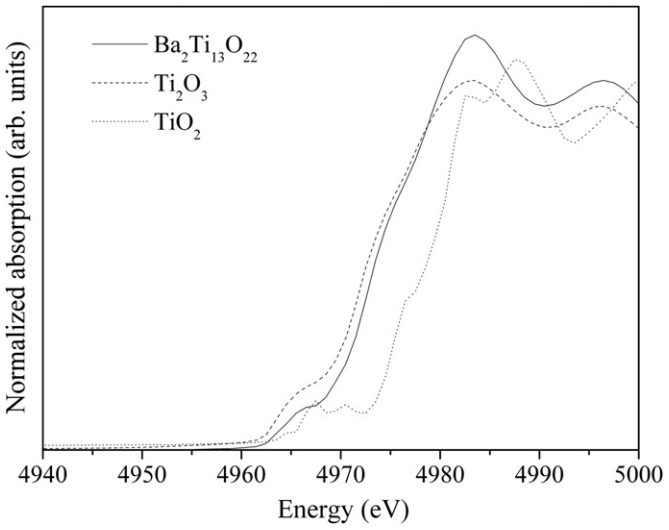

Fig. 1. The Ti K-edge X-ray absorption near edge structure (XANES) spectra of $Ba_2Ti_{13}O_{22}$, Ti_2O_3 and TiO_2. The solid line, broken line and dashed line shows the XANES spectra of $Ba_2Ti_{13}O_{22}$, Ti_2O_3 and TiO_2, respectively.

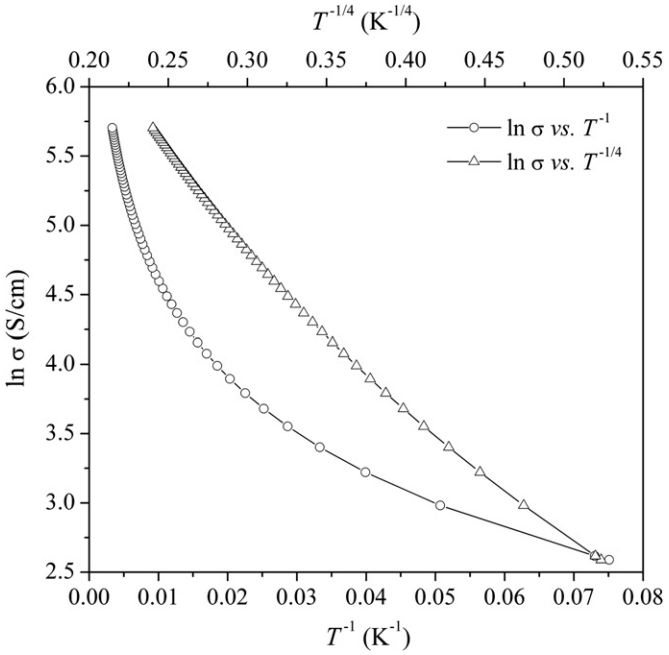

Fig. 2. Temperature dependence of the electrical conductivity of $Ba_2Ti_{13}O_{22}$. A plot of ln σ versus T^{-1} is shown by open circles, and a plot of ln σ versus $T^{-1/4}$ is shown by open triangles.

The result is well consistent with the average Ti–O bond distance in $Ba_2Ti_{13}O_{22}$, as mentioned above.

3.2. Physical properties

Fig. 2 shows the temperature dependence of electrical conductivity for the sintered $Ba_2Ti_{13}O_{22}$ sample. The conductivity of $Ba_2Ti_{13}O_{22}$ at 300 K is approximately 320.50 S/cm, and a semiconducting behavior is observed below room temperature, but the temperature dependence of the conductivity does not obey any activation-type behavior. The conductivity decreases by several orders of magnitude together with the lowering temperature and a pronounced curvature occurs in the Arrhenius plot of T^{-1} (Fig. 2). A similar behavior has been observed for the another

reduced barium titanate $BaTiO_{3-x}$ [3,4]. As one possibility, such a phenomenon is explained as variable range hopping (VRH) based on the Mott–Davis VRH law where logarithmic conductivity shows a liner dependence on $T^{-1/3}$ or $T^{-1/4}$ for two or three dimensional hopping, respectively. Fig. 2 also shows the plot of the logarithm of conductivity ($\ln \sigma$) versus $T^{-1/4}$. The plot is more close to linear that the ($\ln \sigma$) versus T^{-1} plot, but the deviation is quite noticeable. This seems to be consistent with a variable range-hopping in the three-dimensional (3D) system for $Ba_2Ti_{13}O_{22}$. The Seebeck coefficient for the sintered $Ba_2Ti_{13}O_{22}$ sample, measured at 300 K, showed a negative value of -1.25 μV/K, indicating *n*-type behavior.

The temperature dependence of magnetic susceptibility was nearly temperature independent in the range of 60–300 K, which might be due to Van Vleck Paramagnetism. This result was in good agreement with that for the previous single-crystal data [6].

3.3. Electronic structure

Fig. 3 shows the electron density distributions in $Ba_2Ti_{13}O_{22}$ on (100) plane obtained by the FLAPW calculation. A strong covalent bonding feature between the Ti and O atoms is clearly visible in these figures. The average electron density heights at the saddle point between the Ti and O atoms are determined to be 0.57 $Å^{-3}$. It is considered that the covalent bonding of Ti–O was due to the Ti-3*d* and O-2*p* interaction near the Fermi level. On the other hand, the bonding of Ba and O is ionic rather than covalent in character, therefore no bonding is observed around the Ba atoms.

Fig. 4 shows the density of states for $Ba_2Ti_{13}O_{22}$. The origin of energy is at the Fermi level. From this figure, $Ba_2Ti_{13}O_{22}$ is *n*-type semiconductor because the Fermi level is in the conduction band. This fact is in good agreement with the present experimental results by electrical conductivity and thermoelectric power measurements. The valence band of $Ba_2Ti_{13}O_{22}$ in the range from -8.5 to -3.8 eV consists of the O-2*p* orbital hybridized with the Ti-3*d* orbital. The up-spin energy states ranging from -1.5 to 2.3 eV and 2.3 to 5.6 eV are attributed to the t_{2g} states and the e_g states of the Ti-3*d* orbital, respectively. The down-spin energy states ranging from -1.4 to 2.3 eV and 2.3 to 5.6 eV are attributed to the t_{2g} states and the e_g states of the Ti-3*d* orbital, respectively. The band gap value for $Ba_2Ti_{13}O_{22}$ was estimated to be 2.3 eV. From these calculations, it is clearly understood that the Ti orbital and the O orbital decide the band gap.

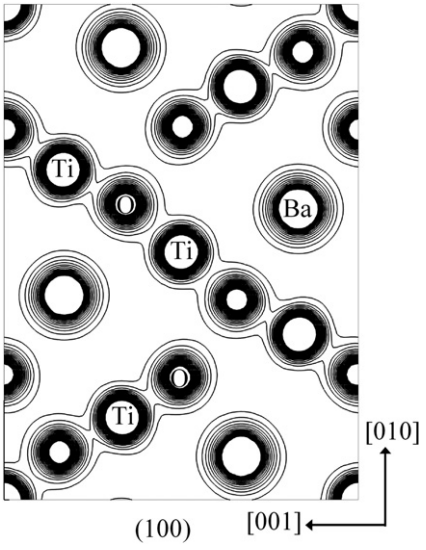

Fig. 3. The electron density distribution in $Ba_2Ti_{13}O_{22}$ on (100) plane obtained by the FLAPW calculation. Contours are drawn from 0.0 to 5.0 $Å^{-3}$ with 0.1 $Å^{-3}$ intervals.

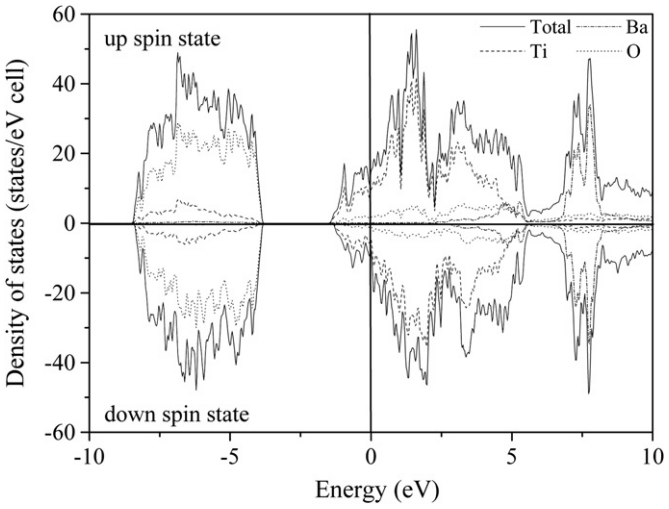

Fig. 4. Density of sates for $Ba_2Ti_{13}O_{22}$.

4. Conclusion

In the present study, the sintered polycrystalline sample of the reduced barium titanate $Ba_2Ti_{13}O_{22}$ was successfully synthesized by solid state reaction at 1523 K in Ar atmosphere for the first time. The electrical conductivity and Seebeck coefficient data showed that $Ba_2Ti_{13}O_{22}$ was an *n*-type semiconductor having potential of three dimensional variable range hopping conductivity. In fact, *n*-type semiconductor was confirmed by the results of the present FLAPW calculations.

Supporting information

The observed, calculated, and difference patterns for the powder XRD Rietveld data of $Ba_2Ti_{13}O_{22}$, crystal structure of $Ba_2Ti_{13}O_{22}$, the connectivity of the TiO_6 octahedral in $Ba_2Ti_{13}O_{22}$, atomic coordinate and isotropic displacement parameters, slected bond length and temperature dependence of the magnetic susceptibility of polycrystalline $Ba_2Ti_{13}O_{22}$ samples.

Acknowledgment

This research was supported by Research Fellowships from the Japan Society for the Promotion of Science for Young Scientists (21-3933).

Appendix A. Supplementary materials

Supplementary materials associated with this article can be found in the online version at doi:10.1016/j.jssc.2011.09.008.

References

[1] D.C. Johnston, J. Low Temp. Phys. 25 (1976) 145.
[2] Y. Takahashi, K. Kataoka, K. Ohshima, N. Kijima, J. Awaka, K. Kawaguchi, J. Akimoto, J. Solid State Chem. 180 (2007) 1020–1027.

[3] D.C. Sinclair, J.M.S. Skakle, F.D. Morrison, R. Smith, T.P. Beales, J. Mater. Chem. 9 (1999) 1327–1331.
[4] K. Kolodiazhnyi, A.A. Belik, S.C. Wimbush, H. Haneda, Phys. Rev. B 77 (2008) 075103-1–075013-5.
[5] S. Möhr, Hk. Müller-Buschbaum, J. Alloys Compd. 199 (1993) 203–206.
[6] J. Akimoto, Y. Gotoh, M. Sohma, K. Kawaguchi, Y. Oosawa, J. Solid State Chem. 113 (1994) 384–392.
[7] J. Schmachtet, Hk. Müller-Buschbaum, Z. Anorg. Allg. Chem. 435 (1977) 243–246.
[8] R.W. Cheary, Acta Crystallogr. Sect. B 46 (1990) 599–609.
[9] T. Höche, P. Olhe, R. Keding, C. Rüssel, P.A. van Aken, R. Schneider, H.-J. Kleebe, X. Wang, A. Jacobson, S. Stemmer, Philos. Mag. 83 (2003) 165–178.
[10] A. Currao, Acta Crystallogr. Sect. C 55 (1999) 2–4.
[11] P. Blaha, K. Schwarz, G. Madsen, D. Kvasnicka, J. Luitz, WIEN2k, Augmented Plane Wave+Local Orbitals Program for Calculating Crystal Properties, Technische Universität Wien, Vienna, 2001.
[12] V.I. Anisimov, F. Aryasetiawan, A.I. Lichtentein, J. Phys.: Condens. Matter 9 (1997) 767–808.
[13] K. Momma, F. Izumi, J. Appl. Crystallogr. 41 (2008) 653–658.